Imaging Algorithm Optimization of Dry Storage Casks Based on Micro-Pattern Gas Detector

LECTURER : YULEI LI , XIAODONG WANG , YI WANG , XIN WEI

EMAIL: LIYULEI@YAHOO.COM

2018-02-23

CONTENTS

1 RESEARCH BACKGROUNDS AND SIGNIFICANCE

brief communications

Radiographic imaging with cosmic-ray muons

Natural background particles could be exploited to detect concealed nuclear materials.

Despite its enormous success, X-ray radiography[1] has its limitations: an inability to penetrate dense objects, the need for multiple projections to resolve three-dimensional structure, and health risks from radiation. Here we show that natural background muons, which are generated by cosmic rays and are highly penetrating, can be used for radiographic imaging of medium-to-large, dense objects, without these limitations and with a reasonably short exposure time. This inexpensive and harmless technique may offer a

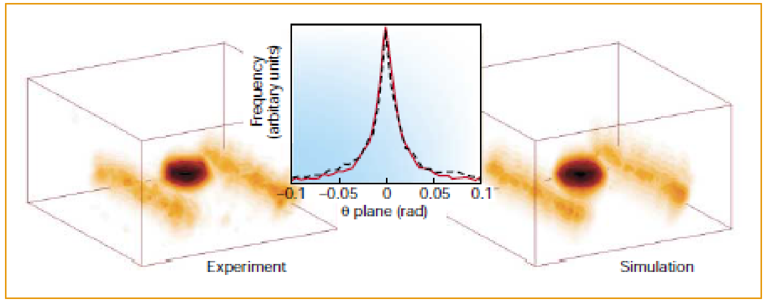

In 2003, "Nature" magazine put forward the concept of scattering imaging using the muon of natural background in the package。

Nature, 2003, 422(6929): 277-277

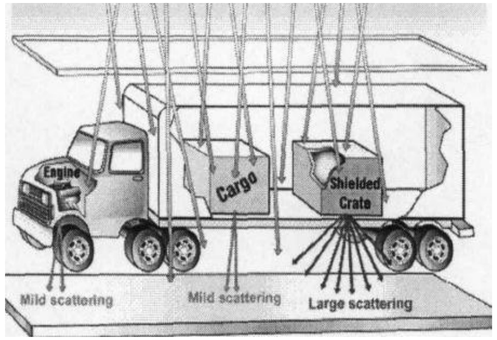

Lausanne Alamos National Laboratory

First Muon Imaging Principle Prototype

- ✓ **No artificial radiation**

The flux is about $1/(cm^2 \cdot min)$

- ✓ **No radiation damage**

Only electromagnetic effect, no nuclear effect

- ✓ **Strong penetration**

Energy distribution in the distribution of 0.1-1000GeV, the average energy of 3-4GeV

Foreign Research Status Quo

(DATA STATISTICS AS OF 2017)

Country	Group	Purpose
Japan	Nagoya University KEK，NEP	Khufu Pyramid Voids Imaging (2017-nature)
Canada	Chalk Reactor Creek Site	Zed-2 Reactor Imaging And Dry Storage Cask Monitoring
France	CEA	Saclay To Tower Imaging
America	Los Alamos	Fukushima Nuclear Accident Simulation (2012-prl)
	Purdue University	Dry Storage Tank Monitoring
Sweden	Uppsala University	Nuclear Fuel Barrel Imaging
Japan	KEK	Reactor Imaging
	Tsukuba University	Reactor Imaging

Research Significance:

I. Check if the reactor core melts under accident conditions.

II. Two-dimensional imaging of heavy nuclear matter in the encapsulated body.

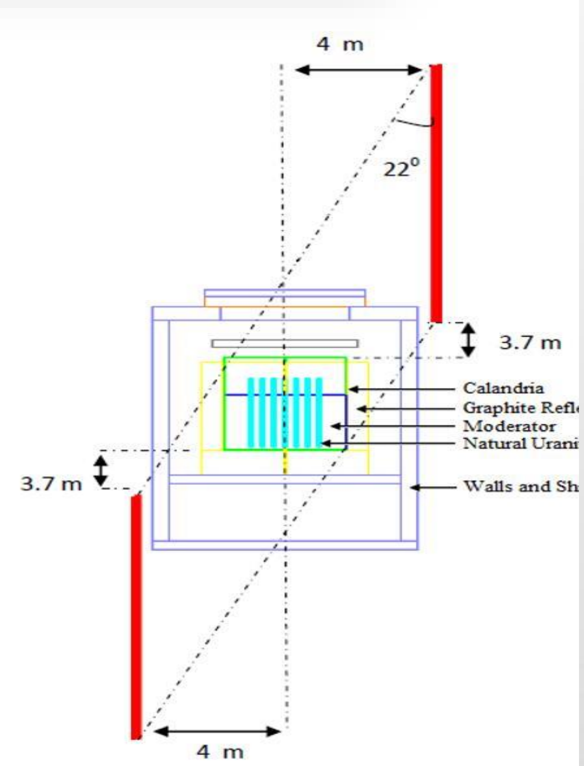

ZED-2 Reactor Bilateral Imaging Structure

Proceedings of the INMM 54th Annual Meeting, Palm Desert, CA, USA, 2013 July 14-18

Application:

- Nondestructive testing of spent fuel dry storage drums
- Imaging in-reactor nuclear fuel assembly
- Imaging the damaged reactor
- Remote monitoring and control reactor core

2 MUON IMAGING FUNDAMENTAL PRINCIPLES

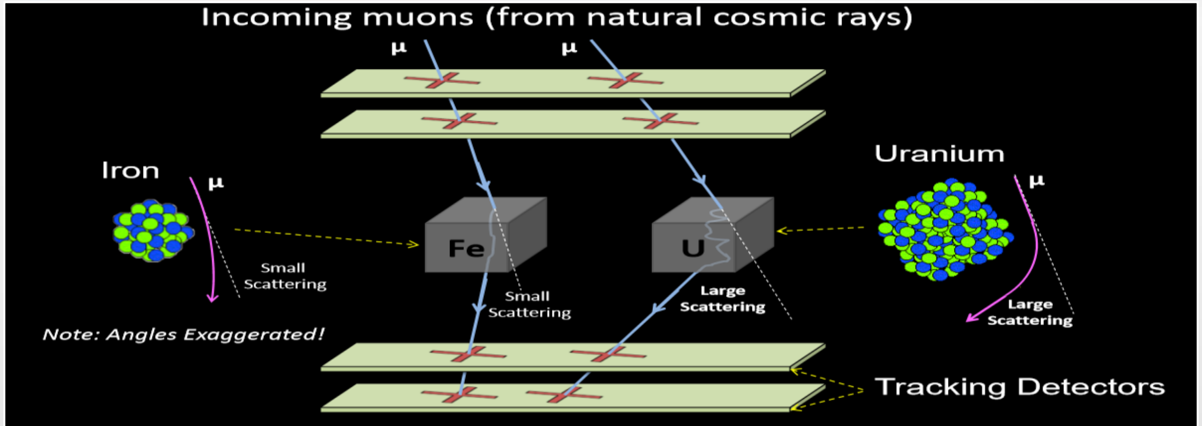

$$\sigma_\theta \cong \frac{15MeV}{\beta cp}\sqrt{\frac{L}{L_{rad}}} \qquad L_{rad} = f\left(\frac{1}{Z}\right)$$

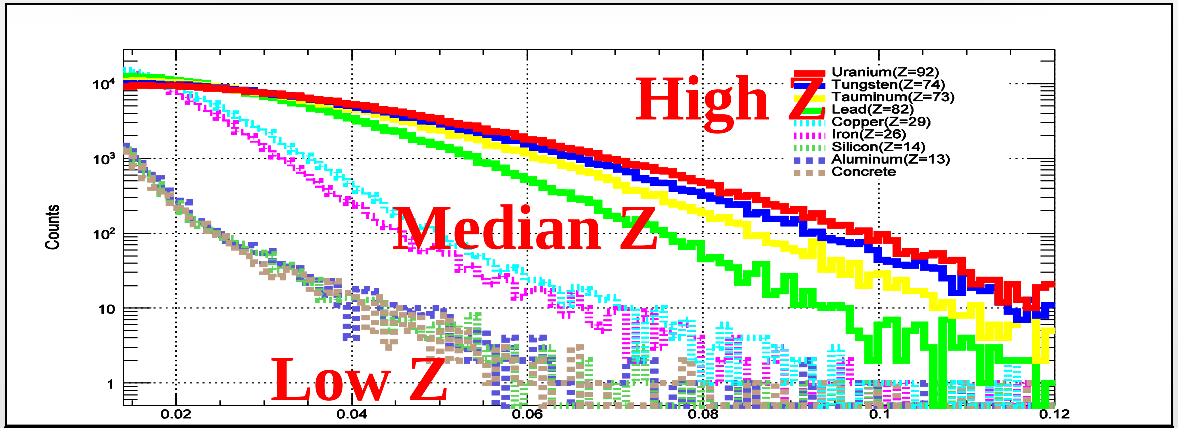

The scattering angle distribution of high, medium and low Z materials has a clear boundary

Muon Multiple Coulomb Scattering (MCS)

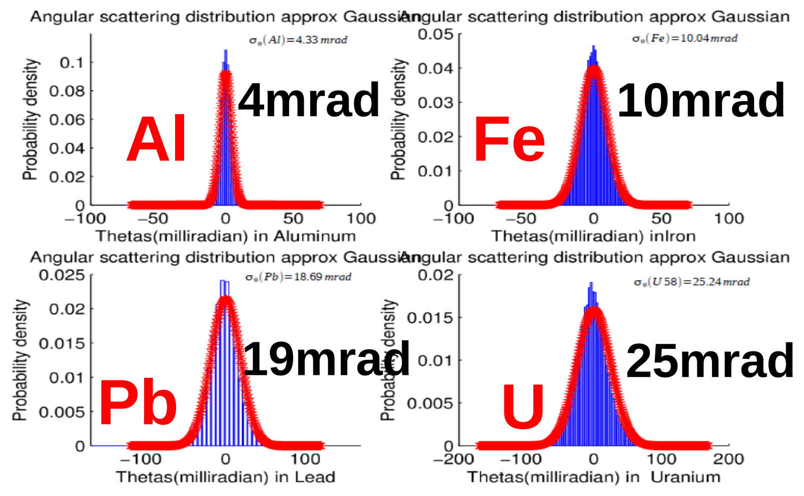

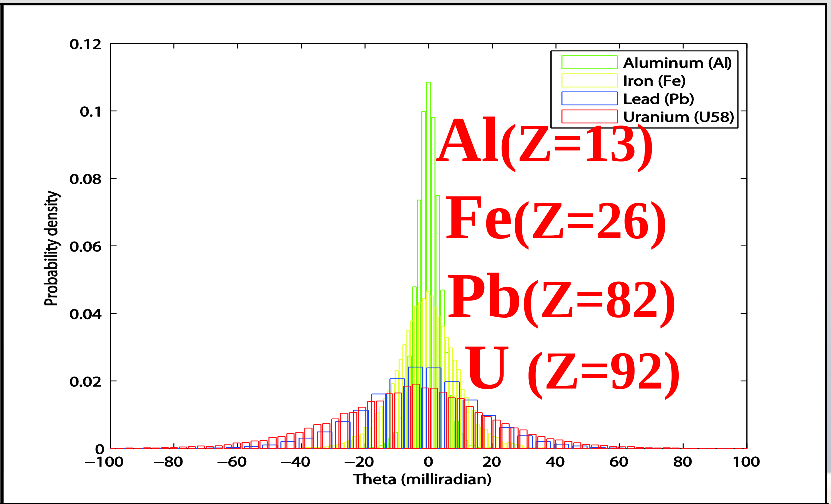

The scattering angle of Muon approximates the Gaussian distribution

Muon Multiple Coulomb Scattering (MCS)

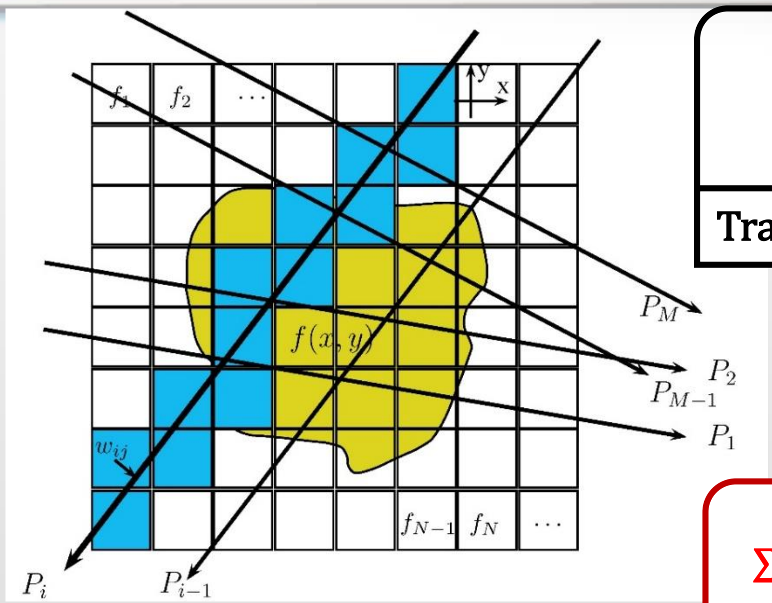

B. Rossi. High Energy Particles,1952.

$$P_i = \sum_j L_{ij} f_j$$

Traditional Tomography

$$\Sigma_i = p_{r,i}^2 \sum_j L_{ij} \lambda_j$$

Object Characteristic Function Lambdaj

$$\sigma_\theta \cong \frac{15MeV}{\beta cp} \sqrt{\frac{L}{L_{rad}}}$$

$$\lambda(L_{\mathrm{rad}}) = \left(\frac{15}{p_0}\right)^2 \frac{1}{L_{rad}}$$

$$\lambda = \left(\frac{p}{p_0}\right)^2 \frac{\sigma_\theta}{L}$$

Scattering density : Standard muons pass through the material per unit thickness, Its scattering angle variance size.

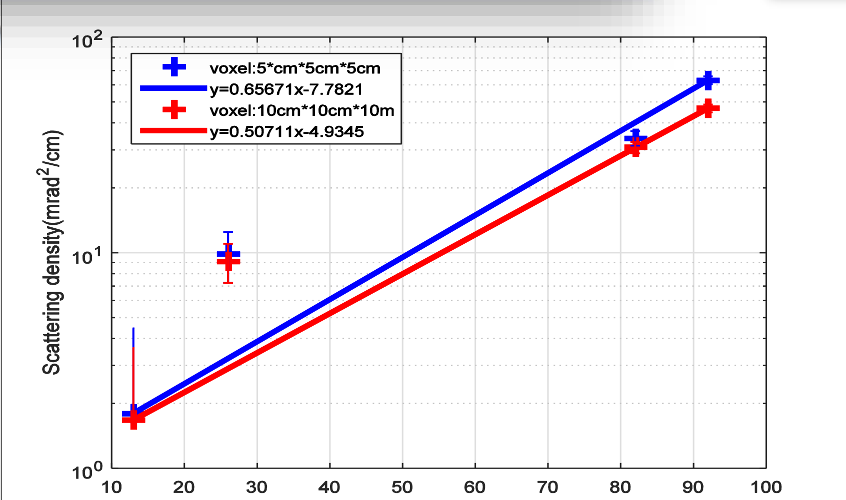

Scattering density is proportional to Z

Clear demarcation of the distribution

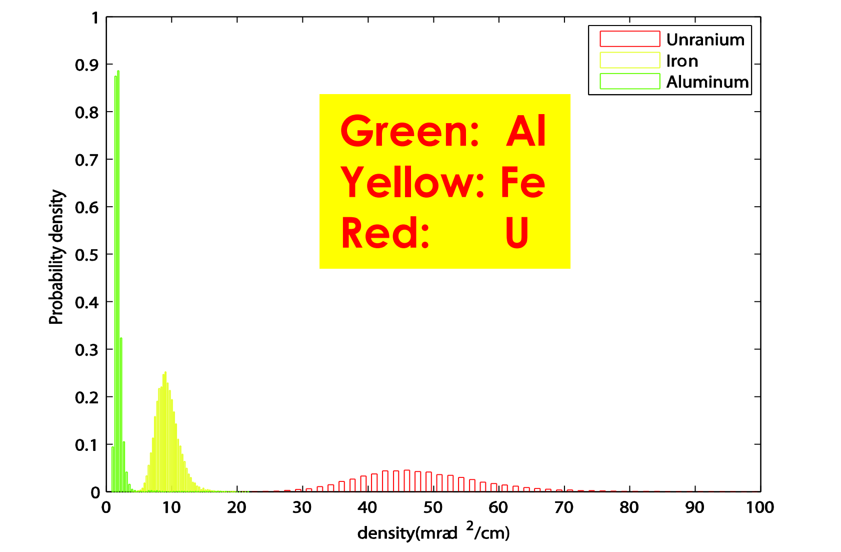

3 RECONSTRUCTION ALGORITHM AND RESULTS

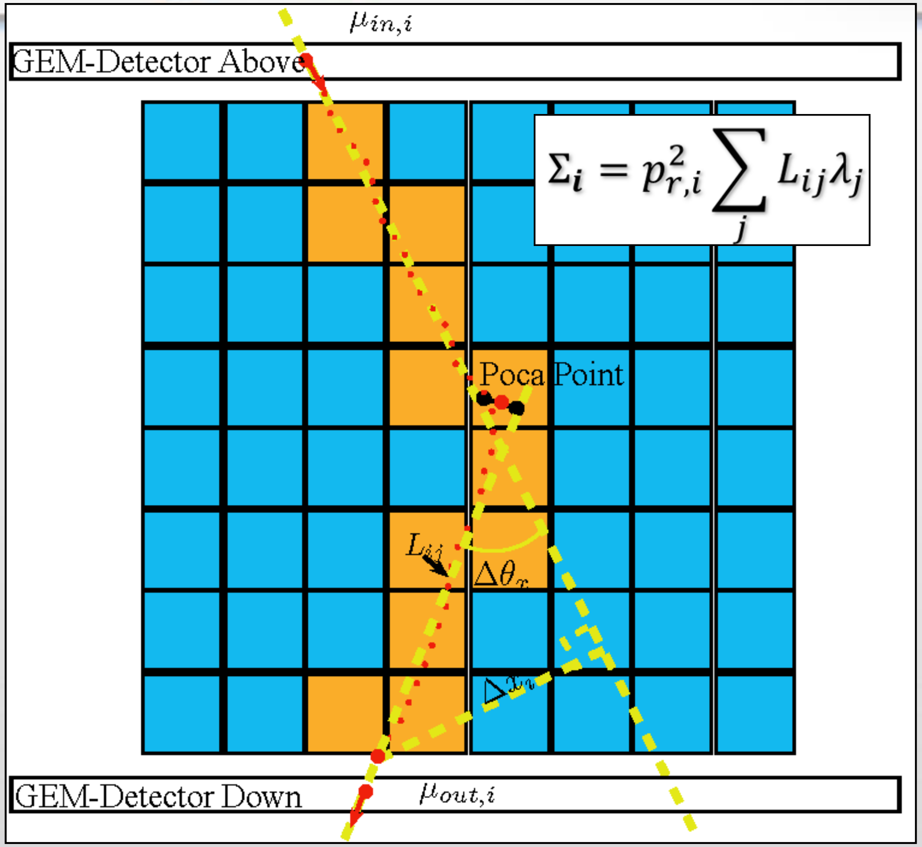

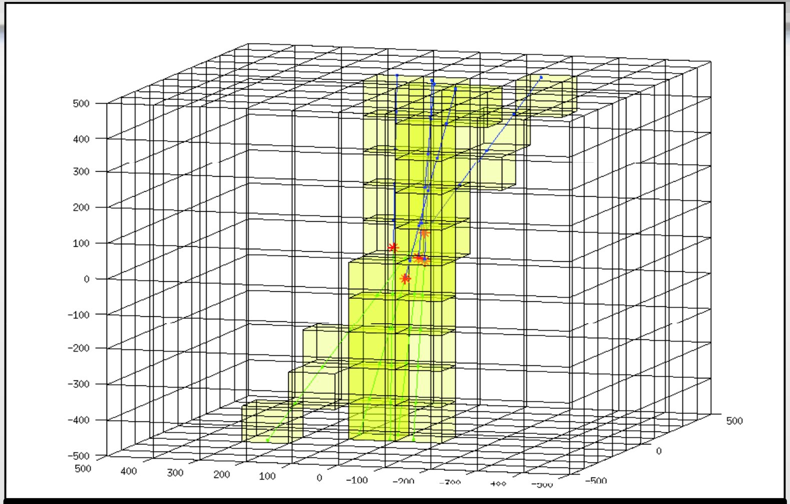

Poca Algorithm Principle

Point Of Closet Approach (PoCA)

Estimates the scattering points by solving the midpoint of the out-of-plane-line to obtain the estimated scattering density of each voxel.

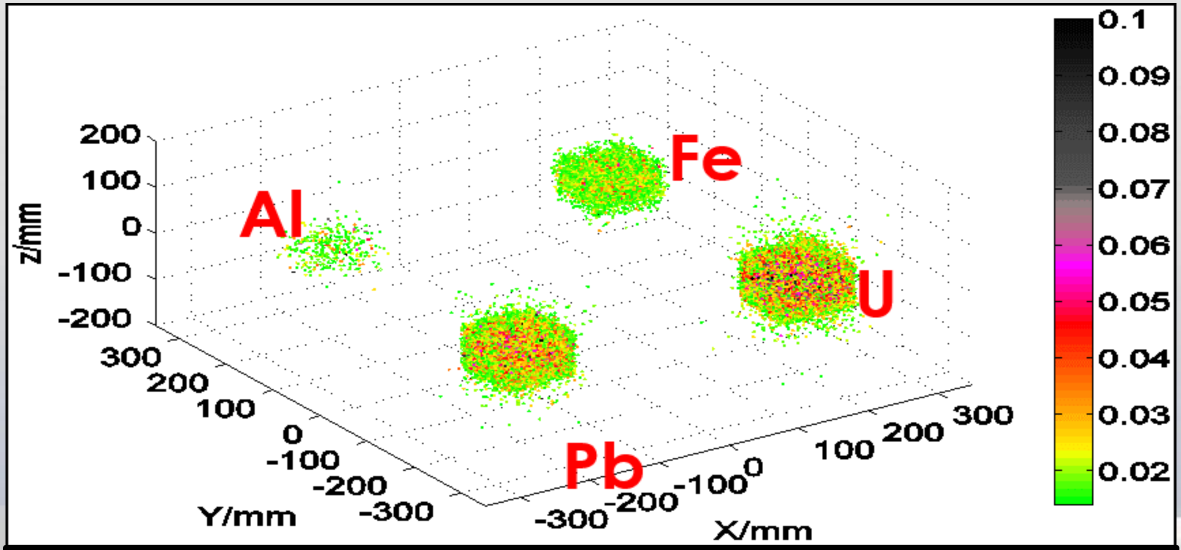

The PoCA algorithm is sensitive to high Z materials

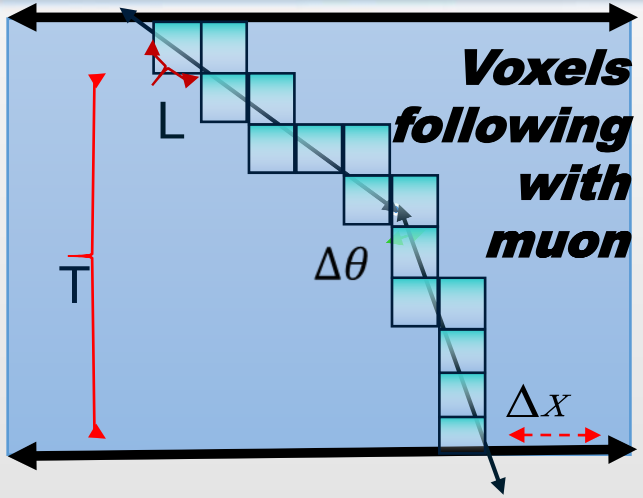

$$MLS: \; D_i = \Delta\theta_i$$

$$MLSD: \; D_i = \begin{bmatrix} \Delta\theta_i \\ \Delta x_i \end{bmatrix}$$

$$\Sigma_i = p_{r,i}^2 \sum_j L_{ij}\lambda_j$$

$$\Sigma_i = p_{r,i}^2 \sum_j W_{ij}\lambda_j$$

$$\begin{bmatrix} L_{ij} & \frac{L_{ij}^2}{2} + L_{ij}T_{ij} \\ \frac{L_{ij}^2}{2} + L_{ij}T_{ij} & \frac{L_{ij}^3}{3} + L_{ij}^2 T_{ij} + T_{ij}^2 L_{ij} \end{bmatrix}$$

Maximum Likelihood Scattering-Expectation Maximization (ML-EM)

Step E: Calculate the conditional probability distribution $P(D, H|\lambda)$ of implicit data H

$$MLS - EM: \; S_{ij} = f\left(L_{ij}, D_i, \Sigma_i, p_{r,i}^2, \lambda_j\right)$$

$$MLSD - EM: \; S_{ij} = f\left(L_{ij}, T_{ij}, D_i, \Sigma_i, p_{r,i}^2, \lambda_j\right)$$

Step M: Maximize the likelihood function and obtain the estimated scattering density λ

$$\lambda_j^{n+1} = \sum_{i:L_{ij}\neq 0} \frac{S_{ij}}{2M_j}$$

$$\lambda_j^{n+1} = \frac{1}{2} median_{i:L_{ij}\neq 0} \cdot S_{ij}$$

Iterates to the distribution of the previous step, iterating until convergent.

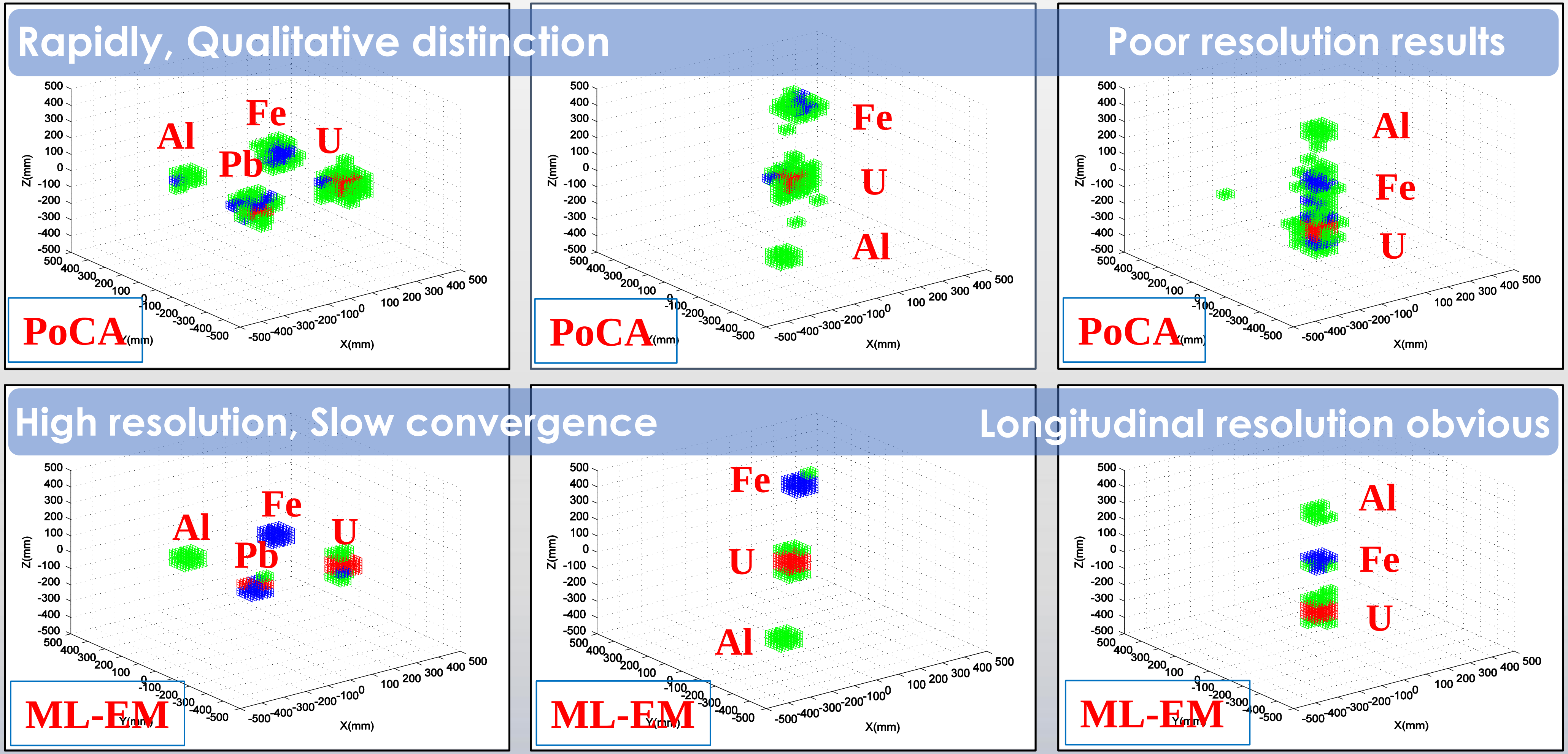

Horizontal imaging | **Diagonal imaging** | **Longitudinal imaging**

ML-EM AND PoCA Results Compared

Use Bayes' rule to get the posterior probability

$$P(D|\lambda) = \frac{P(D|\lambda)P(\lambda)}{P(D)}$$

Add prior knowledge of the constraints

$$p(\lambda) = Ae^{-\beta U(\lambda)}, U(\lambda) = \sum_j V(\lambda_j)$$

Divide the data into ordered subsets for acceleration

$$\lambda_{MAP-OS}^{n+1} = \arg\max_{\lambda}\left(\sum_j \sum_{i\in S_b}\left(-log\lambda_j - S_{ij} / (2\lambda_j)\right)\right) - \beta U(\lambda)$$

The equations for solving the optimal scattering density are iterated each step

$$-\frac{M_j}{\lambda_j} + \sum_{i:L_{ij}\neq o} S_{ij}^n - \beta\dot{V}(\lambda_j) = 0$$

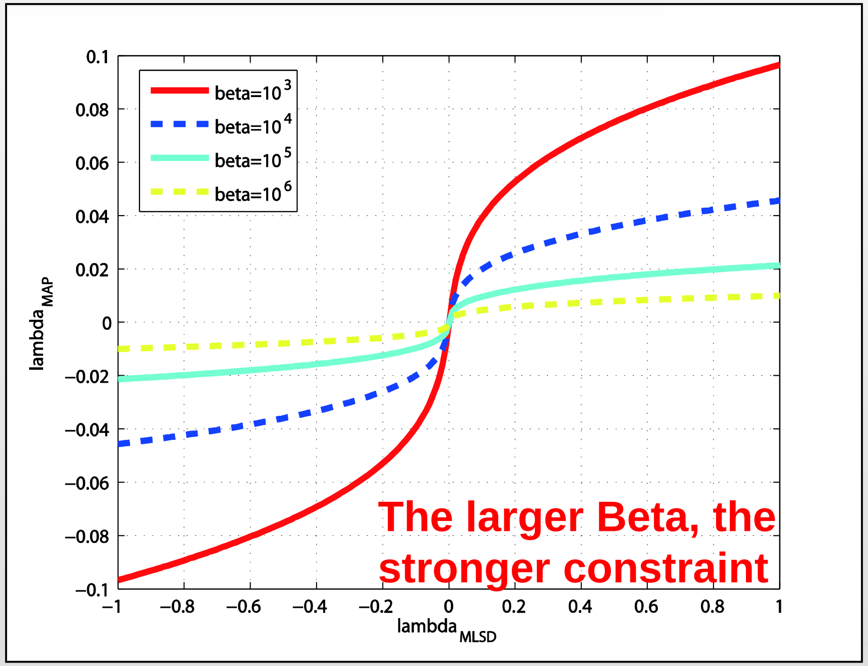

Maximum A Posteriori Probability Ordered Subset Acceleration

MAP-OS

RECONSTRUCTION ALGORITHM AND RESULTS

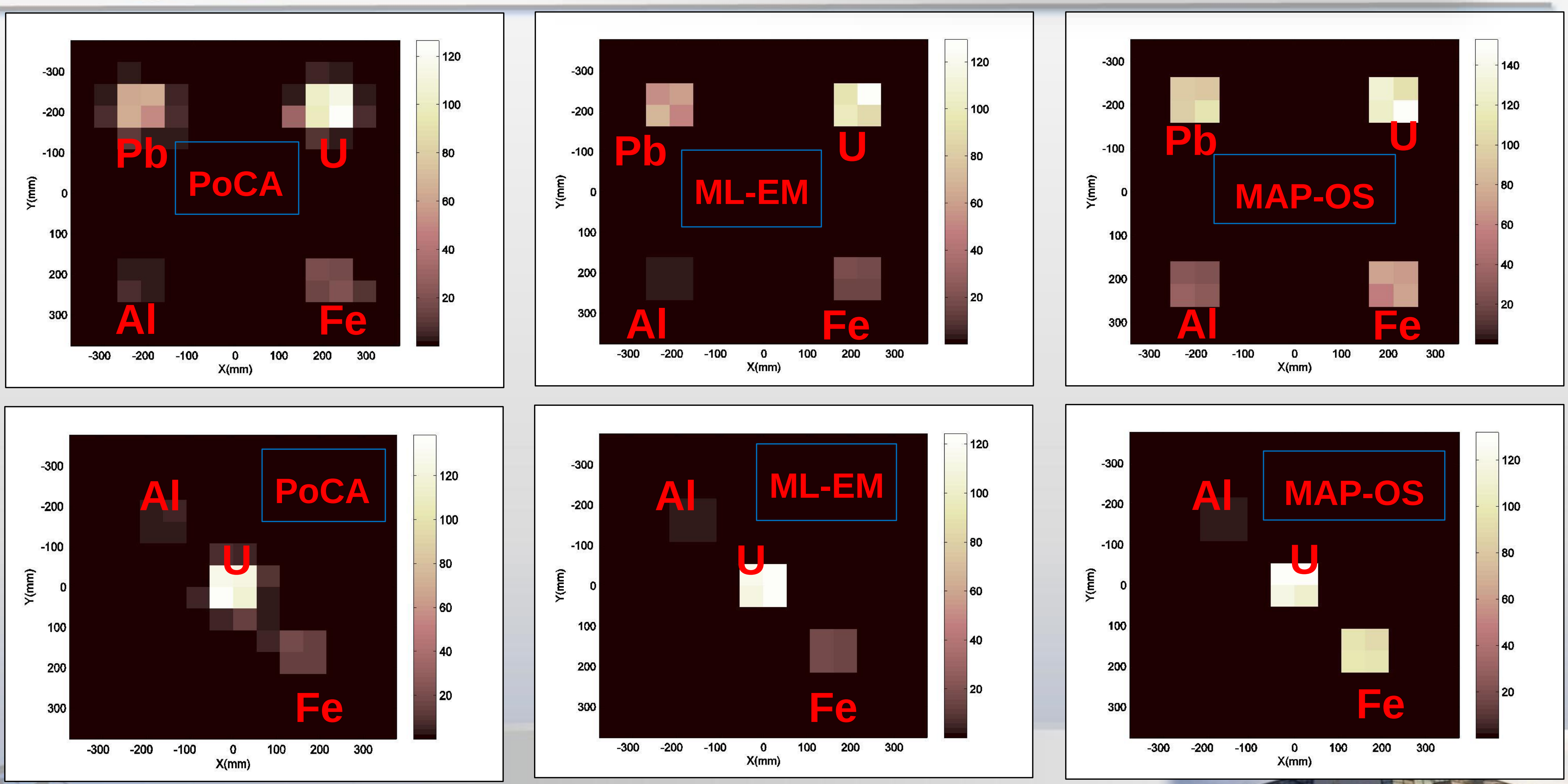

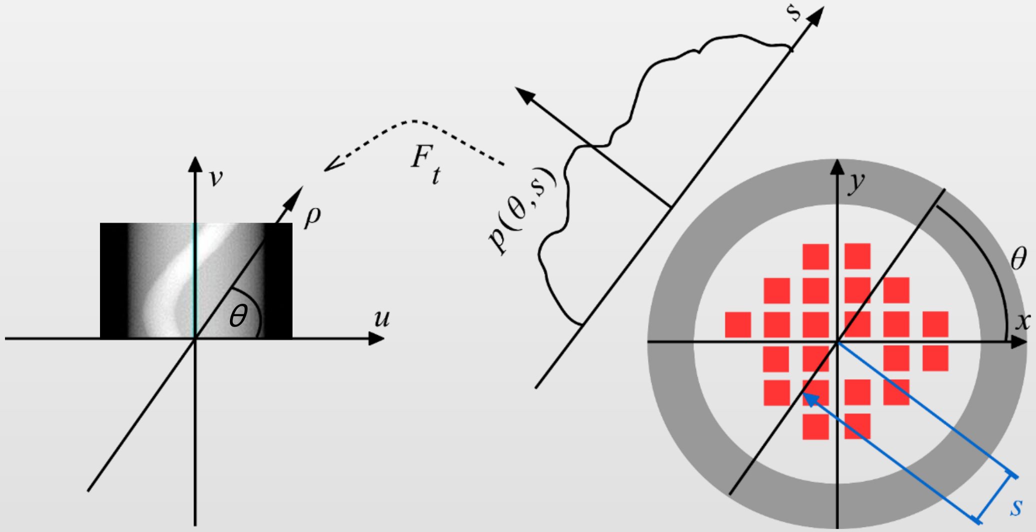

Sinogram: 2D image of projection data at all θ angles.

Projection: The amount of attenuation collected by Muon after it reached the detector through a spent fuel bucket on a path.

Filter Back Projection (FBP)

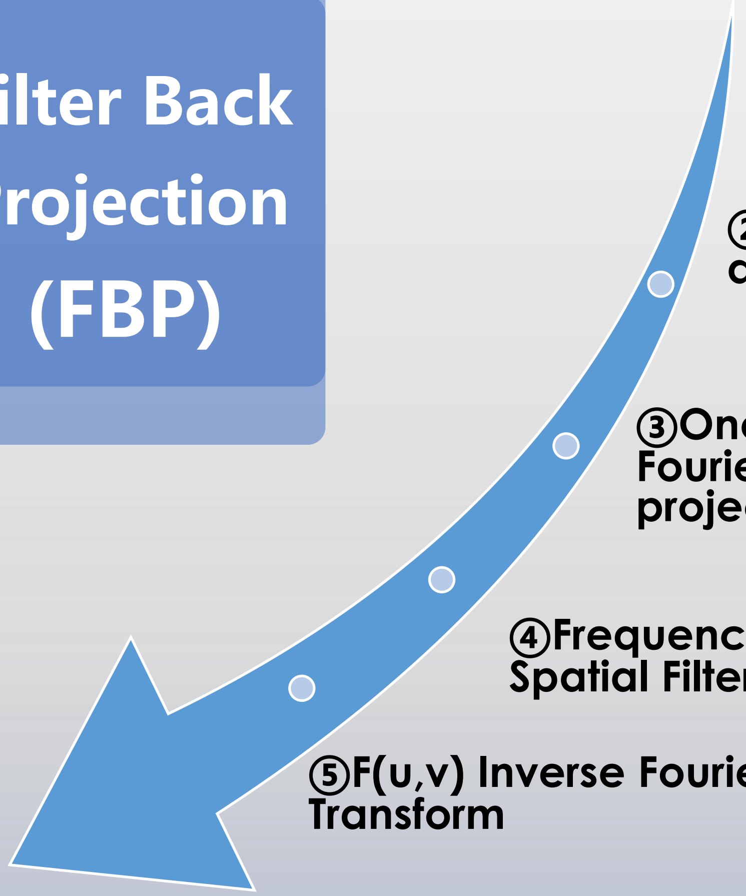

①Characteristic Function *f*(*x*,*y*)

②Projection data of f(x,y)

③One-dimensional Fourier transform of projection data

④Frequency Domain Spatial Filter Processing

⑤F(u,v) Inverse Fourier Transform

⑥Get the eigenfunction image

Four models for building detectors outside dry storage casks

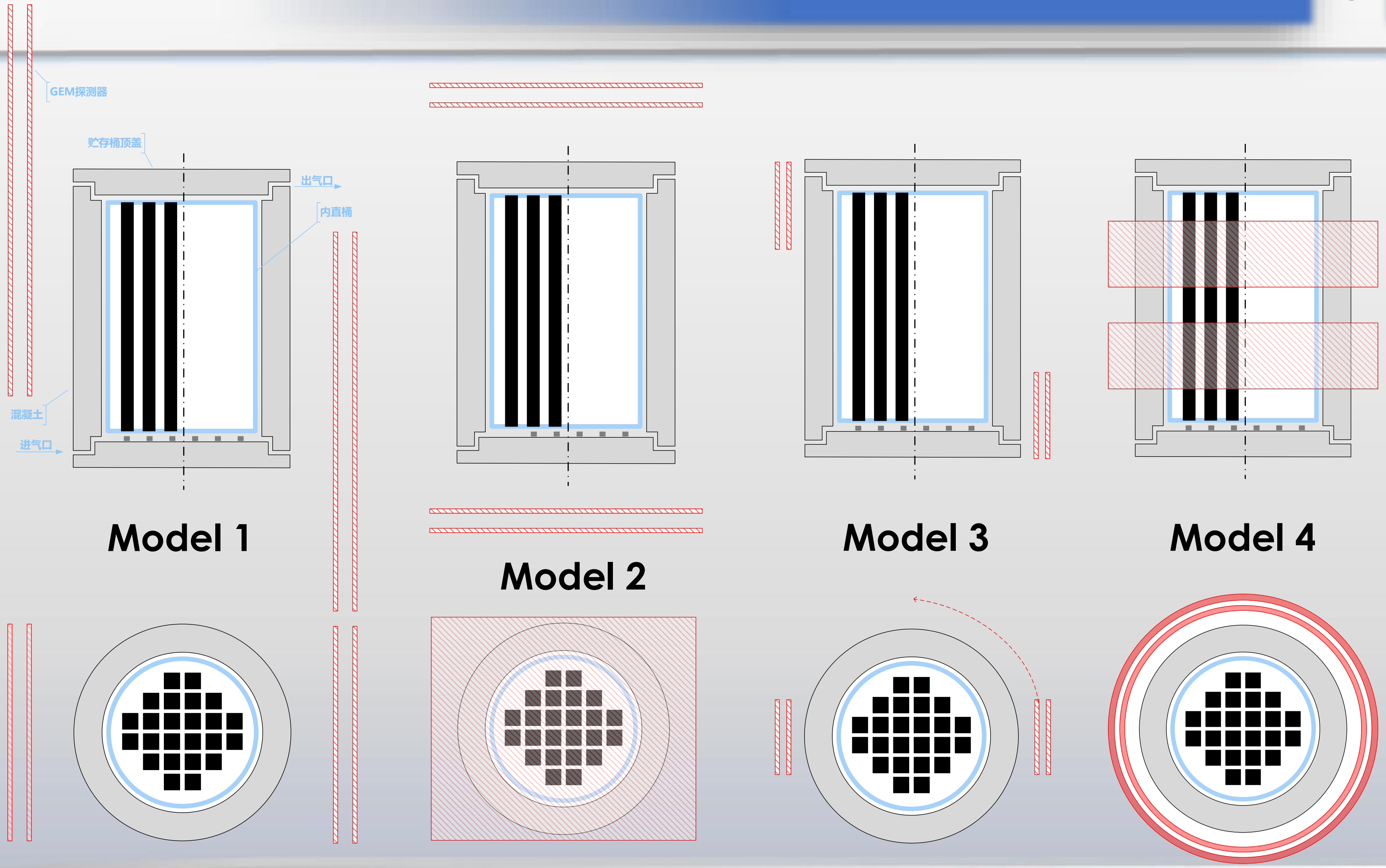

Model 1: Building the detector model on the left and right sides of the dry storage cask using the Geant4

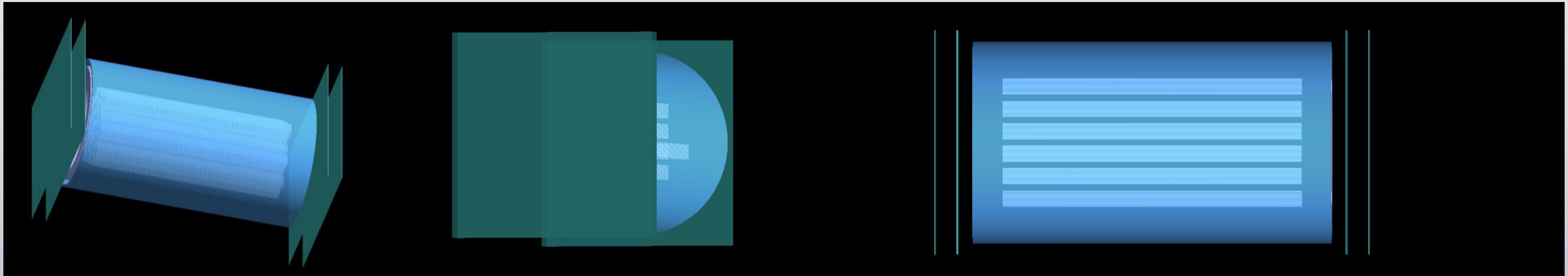

Model 2: Building the detector model on the upper and lower sides of the dry storage cask using the Geant4

The results of simulation imaging of dry storage cask using PoCA algorithm

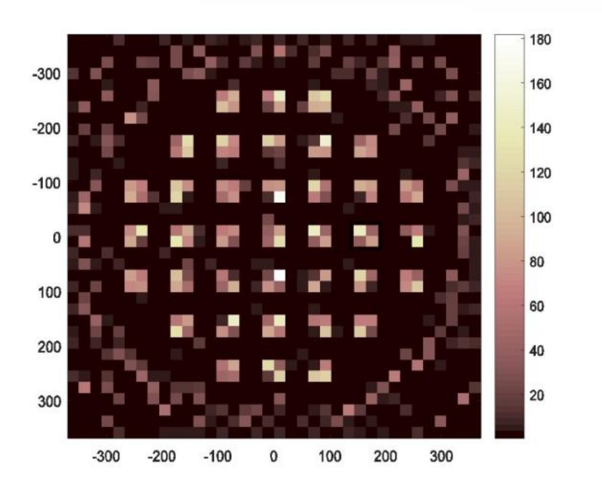

Complete component imaging

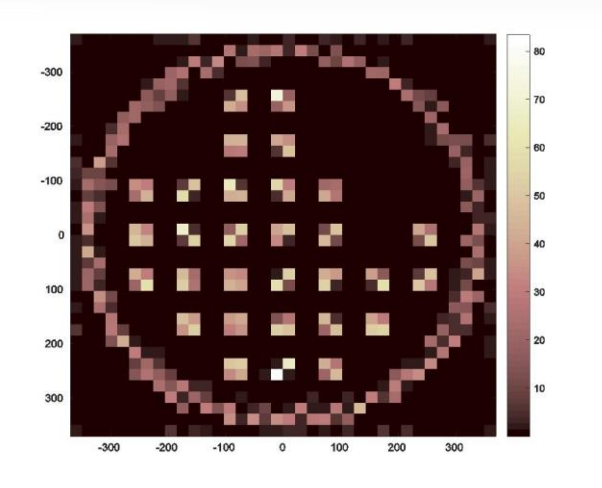

Missing component imaging

Increased positional resolution of 200,300 microns

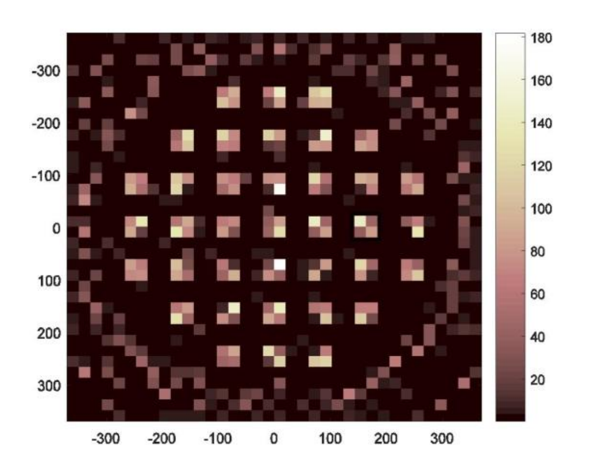

No position resolution

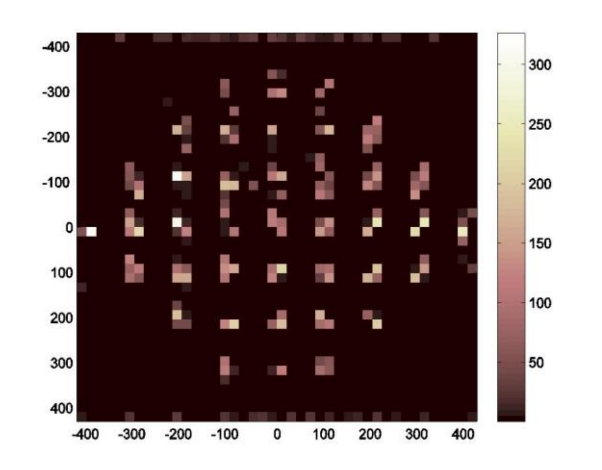

Position resolution 200 microns

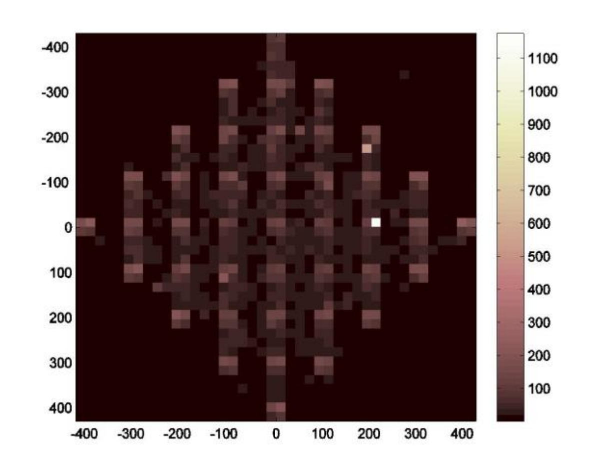

Position resolution 300 microns

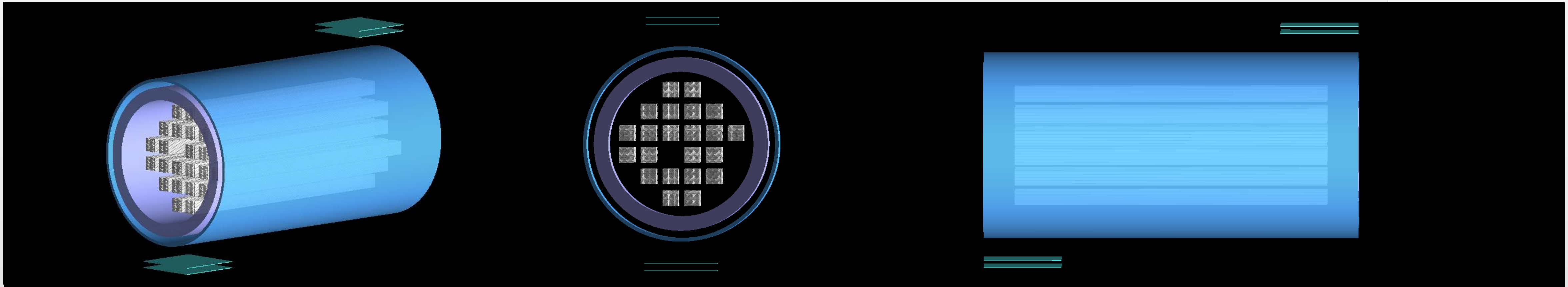

Model 3: Building the miniature detector model on the left and right sides of the dry storage cask using Geant4

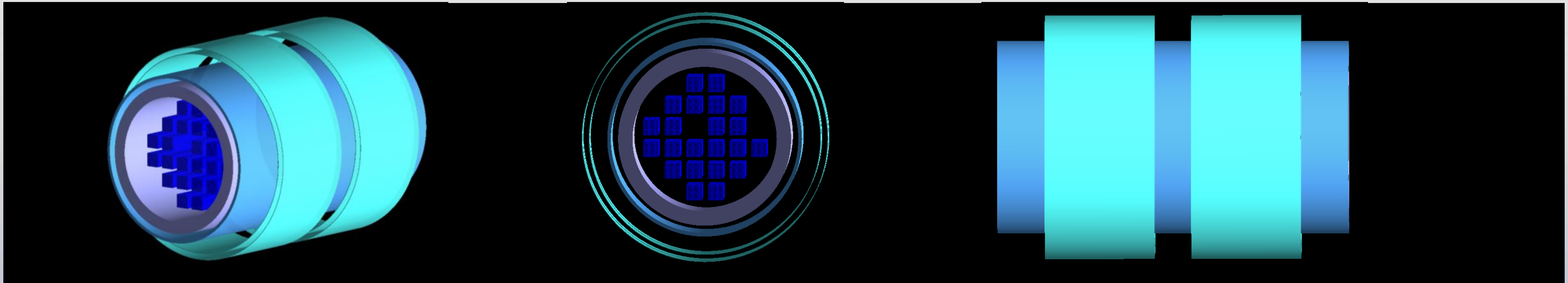

Model 4: Building the ring detector model around the dry storage cask using the Geant4

The results of simulation imaging of dry storage cask using FBP algorithm

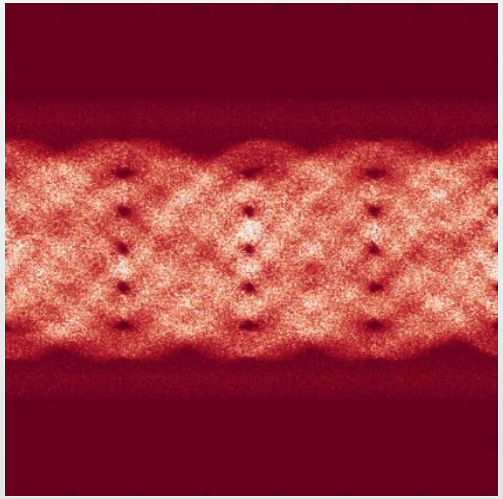

Missing component imaging

Sinogram using FBP

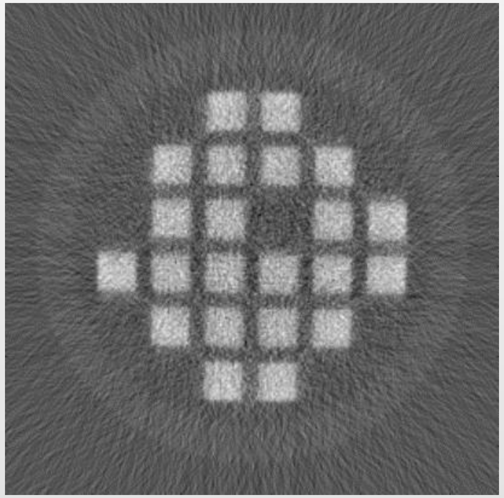

Increased positional resolution of 100, 200,300 microns

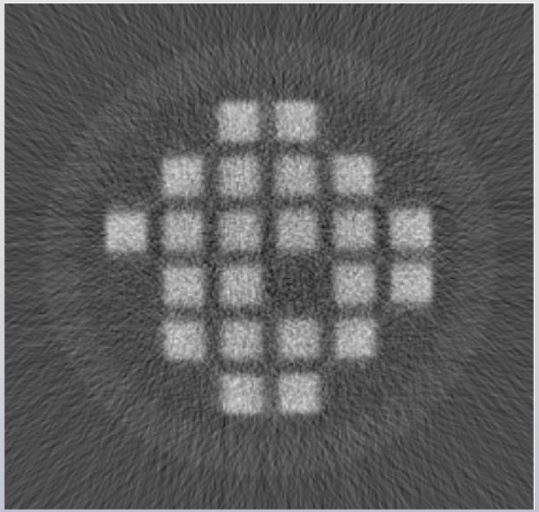

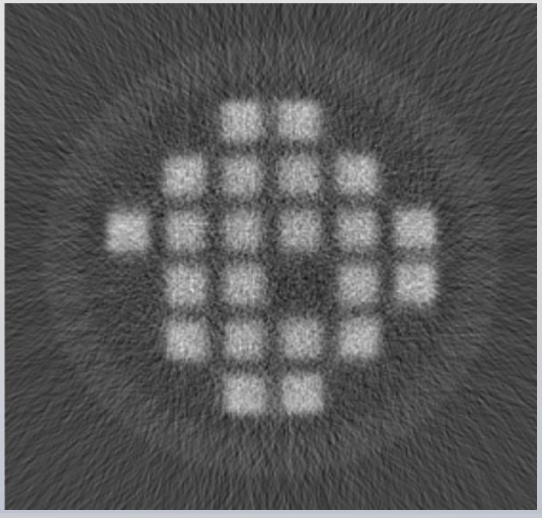

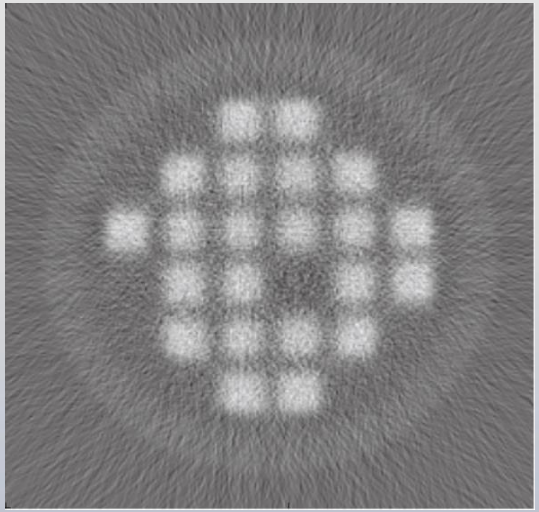

Quantification Process

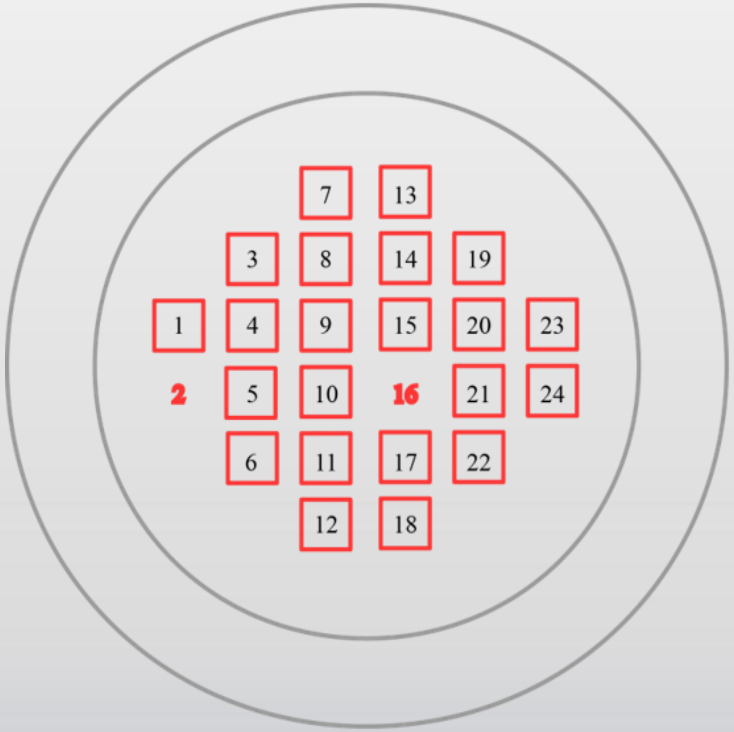

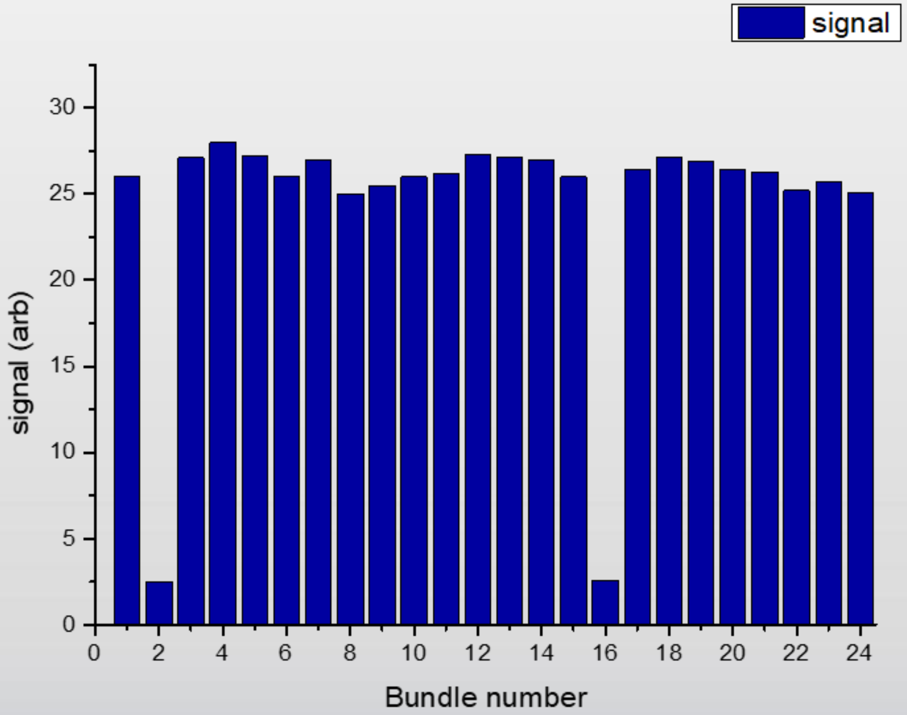

RPC 2018

4 SUMMARY AND FUTURE WORK

SUMMARY

I. The current Muon imaging algorithm is debugged and implemented by Monte Carlo simulation, the results show that:

a. The **PoCA** algorithm can rapidly image, qualitatively discriminate the material but poorly image the longitudinal multilayered object;

b. The **ML-EM** and **MAP-OS** algorithms sharply image the location and structure of matter;

c. The **MAP-OS** algorithm has less iteration time and less memory, and the image smoothing and noise suppression effect is the **best**.

SUMMARY

II. Combining with the algorithm, four models are built for simulation of spent fuel dry storage barrel. Through data simulation and image reconstruction, the results show that:

a. Both solutions based on the **PoCA** algorithm can image missing fuel assemblies but take too long time, and are difficult to operate in view of the problems of oversized gas detectors, high cost, and harsh location conditions.

b. Two optimization schemes based on the **FBP** algorithm can realize the rapid imaging of the material in the barrel, the imaging result is intuitive and the resolution is stronger. The required detector area is small, the location of the conditions is very simple and easy to implement.

Thanks For Your Attention